Behavior-Based Communication-Aware Formation Control in Dynamic Multi-Agent Systems for Jamming Detection and Avoidance

Samuel Peccoud
Department of Electrical and Computer Engineering
Colorado State University
Fort Collins, CO 80521
speccoud@colostate.edu

Sang Xing
Department of Electrical Engineering and Computer Science
Embry-Riddle Aeronautical University
Daytona Beach, FL 32114
xings@my.erau.edu

Tianyu Yang and Richard S. Stansbury
Department of Electrical Engineering and Computer Science
Embry-Riddle Aeronautical University
Daytona Beach, FL 32114
{yang482,stansbur}@erau.edu

***Abstract*—This paper presents a formation control strategy for a swarm of unmanned aerial vehicles (UAVs) that navigate towards a destination while avoiding a jamming area. The proposed approach utilizes a gradient controller for formation control to maximize the communication quality within the swarm. A movement controller is used to go to a destination and avoid a jamming area without prior knowledge of its existence. A simulation is conducted to prove the effectiveness of this approach. The result highlights an efficient navigation strategy while maintaining sufficient communication quality for a multi-agent system.**

***Index Terms*—multi-agent system, formation control, communication-aware, behavior-based, jamming area, obstacle avoidance**

I. Introduction

Unmanned aerial vehicles (UAVs) are being increasingly utilized in various applications, necessitating effective swarm coordination and navigation. In environments where swarms encounter jamming areas, ensuring communication quality and obstacle avoidance becomes paramount [1]. This paper addresses these challenges by proposing a formation control strategy that enables a swarm of UAVs to navigate towards a destination while avoiding a jamming area. The strategy combines a gradient controller, responsible for achieving the desired formation and optimizing communication quality [2], with a movement controller that guides the swarm away from the jamming area and to a destination [3]. The objective is to ensure efficient navigation, maintain swarm communication, and mitigate disruptions caused by the jamming area. The primary contribution of this paper lies in the introduction of a novel formation control strategy tailored for a swarm of unmanned aerial vehicles (UAVs) to successfully navigate towards a predefined destination while avoiding unknown jamming areas.

The gradient controller responsible for achieving the desired formation was first proposed by Li [2]. His approach ensures the swarm maintains a communication standard, but does not consider movement in any fashion limiting its practical use. In reality, UAVs are deployed where there are many hazards preventing the success of missions. Jamming areas or jammers are commonly used to disrupt UAVs due to their reliance on wireless communication [4]. There are many ways to avoid this disruption such as channel surfing, anti-jammer nodes, and spatial avoidance [5]. Spatial avoidance is a commonly used technique because of the enhanced mobility of UAVs [6]. Therefore, it is imperative to develop robust jamming avoidance strategies for UAVs. Xu proposes an approach to navigate such environments with jamming areas but fails to maintain a suitable level of communication quality within the swarm [3]. By combining these two control strategies, a novel approach is derived and tested. The effectiveness of the proposed approach is supported by compelling evidence derived from simulations.

The subsequent sections of this paper are structured as follows. Section II provides a comprehensive overview of the preparatory work required to understand the formation control process. The interaction model at the communication layer is presented in Section III. Section IV outlines the construction of the gradient and movement controllers, which are integrated into the final formation controller model. In Section V, the simulation results are presented, followed by an evaluation of these results in Section VI. Finally, Section VII concludes the paper.

II. Preliminaries

A. System Model

Consider a swarm of n single-integrator modeled agents operating in a two-dimensional space. Each agent's dynamics

are described by

$$\dot{q}_i = z_i, \quad i = 1, 2, \ldots, n, \tag{1}$$

where $q_i, z_i \in \mathbb{R}^2$, $q, z \in \mathbb{R}^{2n}$, and $i \in \mathcal{V}, \mathcal{V} = \{1, 2, \ldots, n\}$,

- q_i denotes the *position input* of i-th agent.
- z_i denotes the *control input* of i-th agent.
- The *formation set* is denoted as $q = \{q_1^\top, q_2^\top, \ldots, q_n^\top\}^\top$.
- The *control set* is denoted as $z = \{z_1^\top, z_2^\top, \ldots, z_n^\top\}^\top$.

B. Graph Theory

Graph theory is a popular method used to model multi-agent systems [7]. A graph G is represented by a pair $(\mathcal{V}, \mathcal{E})$, consisting of a set of vertices $\mathcal{V}$ and a set of edges $\mathcal{E}$. The vertices are typically labeled as $1, 2, \ldots, n$, and the edges are ordered pairs of the vertices, i.e., $\mathcal{E} \subseteq \mathcal{V} \times \mathcal{V}$. Graphs are classified based on their properties. A graph is strongly connected if there exists a path from any vertex to any other vertex. An undirected graph satisfies $(i, j) \in \mathcal{E} \Leftrightarrow (j, i) \in \mathcal{E}$. In a connected graph, the number of connected edges for any vertex is at most $n - 1$ [8]. The set of neighbors of a vertex i is defined as $N_i = \{j \in \mathcal{V} : (i, j) \in \mathcal{E}\}$.

C. Rigid Formation

The control of rigid body formations in a distributed manner has been extensively studied by researchers, often employing concepts from graph rigidity theory and artificial potential fields [9]. In a rigid formation, inter-agent distances are maintained constant throughout the motion. The relative position vector between agent i and agent j is denoted as $\vec{q}_{ij} = q_i - q_j$ [10], and the relative distance is given by

$$r_{ij} = \sqrt{(x_i - x_j)^2 + (y_i - y_j)^2} = \|q_i - q_j\|, \tag{2}$$

where x_i, and y_i represent the coordinates of agent i. To reduce communication complexity and potential errors, a communication range R is introduced. Within the communication range, the neighboring set of agent i is defined as $N_i = \{j \in \mathcal{V} \mid r_{ij} \leq R\}$. Fig. 1 illustrates the neighboring set.

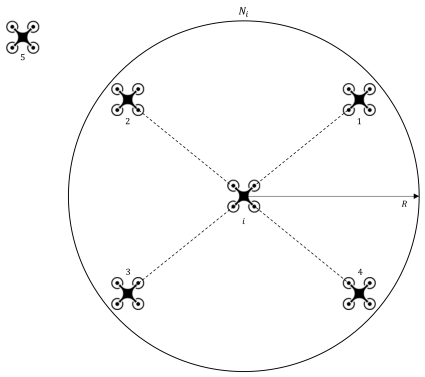

Fig. 1. Agent i and its neighbors in a circle neighborhood

III. Communication Layer

A. Antenna Far-field Propagation

Within a mobile ad hoc network, communication quality is influenced by various factors [11]. To assess channel quality, the concept of outage probability is introduced, representing the probability that the instantaneous Signal-to-Noise Ratio (SNR) falls below a specified threshold [12]. The outage probability can be expressed as a function of system parameters (α), the desired data rate (δ), path loss exponent (v), the reference distance (r_0), and the Euclidean distance between transmitter and receiver (r).

$$P_{\text{out}} = 1 - \exp\left(-\alpha\big(2^\delta - 1\big)\left(\frac{r}{r_0}\right)^v\right). \tag{3}$$

In contrast, the reception probability quantifies the likelihood of accurate information reception in a single input single output (SISO) communication link. It complements the outage probability and characterizes the quality of the communication link in the antenna's far field. By considering the inter-agent distance, the reception probability can be modeled as

$$P_{\text{recep}} = 1 - P_{\text{out}} = \exp\left(-\alpha\big(2^\delta - 1\big)\left(\frac{r}{r_0}\right)^v\right). \tag{4}$$

Moreover, the reception probability captures the quality of the communication link a_{ij} between agent i and agent j in the antenna's far field:

$$a_{ij} = \exp\left(-\alpha\big(2^\delta - 1\big)\left(\frac{r_{ij}}{r_0}\right)^v\right) = \exp\left(-\beta\left(\frac{r_{ij}}{r_0}\right)^v\right), \tag{5}$$

where $\beta = \alpha\big(2^\delta - 1\big)$.

The reception probability, as described by the channel quality model, inversely correlates with the inter-agent distance. Here, the notion of communication range aligns with the reception probability threshold. Thus, within the communication range R, the set of neighbors for agent i can be defined based on the reception probability threshold P_T. The neighboring set is now denoted as

$$N_i = \{j \in \mathcal{V} \mid a_{ij} \geq P_T\}. \tag{6}$$

Incoming packets from agents outside this set are discarded due to their lower reception probabilities.

B. Antenna Near-field Propagation

The antenna near-field refers to the region in close proximity to the antenna, and its boundary with the antenna far-field is defined by the reference distance r_0 [13]. To strike a balance between accuracy and simplicity, an approximate model g_{ij} is commonly employed to capture near-field signal propagation.

$$g_{ij} = \frac{r_{ij}}{\sqrt{r_{ij}^2 + r_0^2}}. \tag{7}$$

The simplified model, denoted by equation (7), represents the near-field channel quality as a function of the inter-agent distance. As the distance between agents approaches zero, the channel quality diminishes, and vice versa.

C. Communication-aware Interaction Model

To capture the combined effects of signal scattering, interference, and path loss in both the antenna near-field and far-field regions, a communication-aware interaction model is introduced by Li [2]. The model, denoted in equation (8), incorporates the near-field propagation factor g_{ij} and the far-field reception probability a_{ij} as follows:

$$\phi\left(r_{ij}\right)=g_{ij}\cdot a_{ij}=\frac{r_{ij}}{\sqrt{r_{ij}^{2}+r_{0}^{2}}}\cdot\exp\left(-\beta\left(\frac{r_{ij}}{r_{0}}\right)^{v}\right). \quad (8)$$

The objective is to identify the optimal inter-agent distance r_{ij}^{*} that maximizes communication performance. Deviating from this optimal distance, whether larger or smaller, results in reduced communication quality. To find the maximum performance, we take the first-order derivative of equation (8) with respect to r_{ij}, denoted as:

$$\frac{d\phi}{dr_{ij}}=\varphi(r_{ij}), \quad (9)$$

where

$$\varphi(r_{ij})=\frac{-\beta v(r_{ij})^{v+2}-\beta v r_{0}^{2}(r_{ij})^{v}+r_{0}^{v+2}}{\sqrt{(r_{ij}^{2}+r_{0}^{2})^{3}}}\cdot\exp\left(-\beta\left(\frac{r_{ij}}{r_{0}}\right)^{v}\right). \quad (10)$$

For a multi-agent system, Li's model enhances our understanding of inter-agent communication quality.

IV. Control Layer

A. Gradient Controller

An artificial potential function denoted as $\psi(r_{ij})$ is introduced to model the interaction between agent i and agent j. This potential function possesses several important properties including non-negativity, continuous differentiability, and a strict minimum at a specific distance r_{α} [2].

The potential function encodes a desired rigid formation with the target distance r_{α}. To achieve distributed rigid formation control, a gradient-based control law is employed, which is formulated as the negative gradient of the local potential functions,

$$\mathcal{G}_{i}=-\nabla_{q_{i}}\left[\sum_{j\in N_{i}}\psi(r_{ij})\right]. \quad (11)$$

The pairwise potential function is defined as

$$\psi_{t}\left(r_{ij}\right)=\begin{cases}\psi\left(r_{ij}\right), & \forall(i,j)\in\mathcal{E},\\ \psi(R) & \text{otherwise.}\end{cases}, \quad (12)$$

to evaluate the interaction between all pairs of agents. Drawing inspiration from the concept of the artificial potential function, a gradient-based controller is devised. The controller is expressed as

$$\mathcal{G}_{i}=\sum_{j\in N_{i}}\left[\varphi(r_{ij})\cdot e_{ij}\right], \quad (13)$$

where $e_{ij}=(q_{i}-q_{j})/\sqrt{1+r_{ij}}$ is the unit vector pointing from agent j to agent i. This gradient-based controller leverages the communication-aware interaction model to guide agents toward the desired formation while taking into account the optimal inter-agent communication distances.

B. Movement Controller

1) Move to Destination: As described by Xu in [3], to make an agent go from a starting location to a destination location it is assigned a vector. We adapted this method to each agent in the swarm as seen in Fig 2, and adapted the destination vector (14). The destination coordinates are predetermined, and they are shared by all the agents. Assume (x_i, y_i) represent an agent's position, and $(x_{\text{dest}}, y_{\text{dest}})$ represent the destination's coordinates. The destination vector is defined as

$$V_{\text{move\_to\_destination}}=\frac{1}{\sqrt{\left(x_{\text{dest}}-x_{i}\right)^{2}+\left(y_{\text{dest}}-y_{i}\right)^{2}}}\times\begin{bmatrix}x_{\text{dest}}-x_{i}\\ y_{\text{dest}}-y_{i}\end{bmatrix}. \quad (14)$$

f_1 in (15) denotes a control parameter that scales the direction vector. a_m and b_m are adjustable constants that alter the movement behavior. The distance from an agent to the destination is d_m. f_1 is given by

$$f_{1}\left(d_{m}\right)=\begin{cases}a_{m}, & d_{m}\in(b_{m},+\infty)\\ a_{m}\frac{d_{m}}{b_{m}}, & d_{m}\in[0,b_{m}]\end{cases}. \quad (15)$$

Fig 2 is a simulation where a swarm moves to a destination. Initially, the agents are placed randomly in the same general area far from the destination. Roughly halfway through the simulation, the swarm approaches the destination, while the gradient controller simultaneously organizes the swarm to maximize communication quality. The final positions show that even though each agent in the swarm is moving to the same destination, the gradient controller forces an optimal formation with the centroid of the swarm in the destination square.

TABLE I
Control Parameters for Fig 2

a_m	b_m
0.1	1.0

2) Avoid Jamming Area: To have the swarm avoid a jamming area, each agent avoids the closest known jamming location $(x_{\text{jam}}, y_{\text{jam}})$. This formulation of the problem is very similar to obstacle avoidance problems [3]. In the scenario where a communication link intersects the jamming area, the communication quality index $\phi\left(r_{ij}\right)$ experiences a reduction of 75%. As a consequence, the resulting value falls well below the threshold P_T, effectively simulating a realistic jamming event and leading to the disruption of the communication link between agent i and agent j. If an agent fully enters the jamming area, all communication links associated with that agent would be lost, resulting in isolation. Traditionally, moving backward is a common approach to evade jamming areas or obstacles; however, this method can lead to deadlocks.

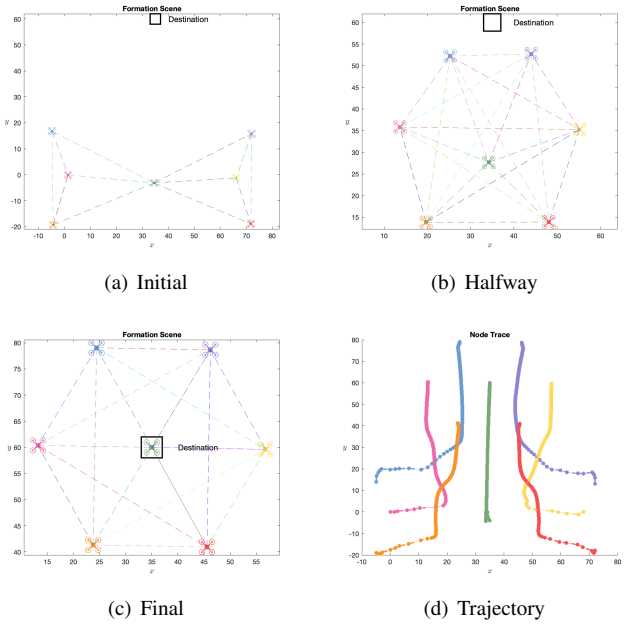

(a) Initial (b) Halfway

(c) Final (d) Trajectory

Fig. 2. Simulation of 7 UAVs traveling towards and stopping at a specified destination.

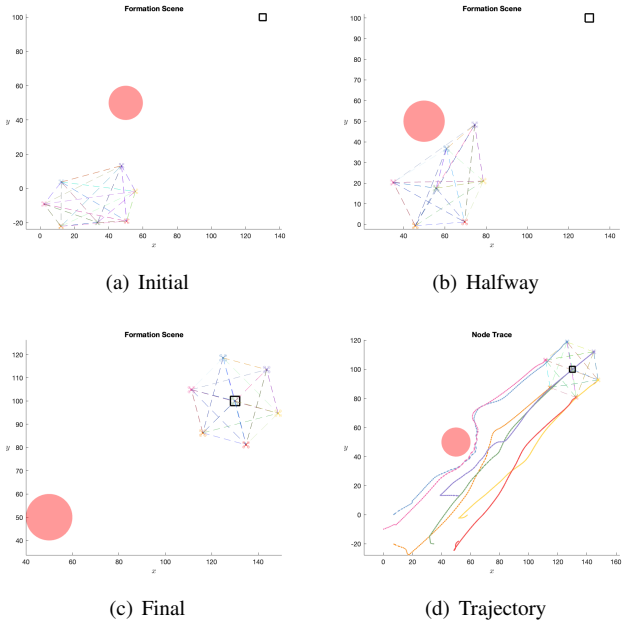

(a) Initial (b) Halfway

(c) Final (d) Trajectory

Fig. 3. Simulation of 7 UAVs avoiding a jamming area while traveling towards the destination.

To address this issue, an alternative strategy known as the jamming avoidance vector is employed. The jamming avoidance vector denoted as $V_{\text{jamming\_avoidance}}$, alters the agent's movement direction by 90 degrees relative to the jamming area. It is defined as follows:

$$V_{\text{jamming\_avoidance}} = \frac{1}{\sqrt{\left(x_{\text{jam}} - x_i\right)^2 + \left(y_{\text{jam}} - y_i\right)^2}} \times \begin{bmatrix} \pm\left(y_{\text{jam}} - y_i\right) \\ \mp\left(x_{\text{jam}} - x_i\right) \end{bmatrix}. \tag{16}$$

The $\pm$ sign of this vector determines whether the agents will turn right or left to avoid a jamming location.

Additionally, control parameter $f_2\left(d_0\right)$ activates the jamming avoidance behavior based on the distance d_0 between the agent and the jamming area. The control parameter is defined as:

$$f_2\left(d_0\right) = \begin{cases} 0, & d_0 \notin \left[b_f, b_0\right] \\ a_0\left(\frac{d_0}{b_f - b_0} + \frac{b_0}{b_0 - b_f}\right), & d_0 \in \left[b_f, b_0\right] \end{cases}, \tag{17}$$

where b_f and b_0 are adjustable parameters determining the range where the jamming avoidance behavior is triggered [14]. a_0 is an adjustable parameter controlling the strength of the avoidance behavior. Fig 3 provides a simulation utilizing (14) through (17) for a swarm of seven agents to avoid a jamming area.

TABLE II
CONTROL PARAMETERS FOR FIG 3

a_m	b_m	a_0	b_0	b_f
0.1	1.0	0.6	20.0	0.0

3) Follow Jamming Area Edge: In scenarios where the jamming area is large, the swarm needs to follow the edge of the jamming area. To achieve this behavior, the swarm employs an edge-following strategy. The edge-following vector, denoted as $V_{\text{follow\_edge}}$, is calculated similarly to the avoidance vector.

The edge-following behavior can be represented by the following equation:

$$V_{\text{follow\_edge}} = \frac{1}{\sqrt{\left(x_{\text{jam}} - x_i\right)^2 + \left(y_{\text{jam}} - y_i\right)^2}} \times \begin{bmatrix} \pm\left(y_{\text{jam}} - y_i\right) \\ \mp\left(x_{\text{jam}} - x_i\right) \end{bmatrix}, \tag{18}$$

where x_{jam} and y_{jam} represent the coordinates of the jamming area, and x_i and y_i represent the coordinates of the i-th agent. The $\pm$ sign of this vector acts the same as the avoidance vector.

The function $f_3\left(d_0\right)$ determines the magnitude of the edge-following vector based on the agent's proximity to the jamming area. This function is defined as:

$$f_3\left(d_0\right) = \begin{cases} 0, & d_0 \notin \left[0, e_f\right] \\ a_f, & d_0 \in \left[0, e_f\right] \end{cases}, \tag{19}$$

where d_0 represents the distance between an agent and the jamming area, e_f is a predefined threshold distance, and a_f is the force applied to the agent when within the threshold distance. The edge of a jamming area is simulated as points in Fig 4, where a swarm of seven agents, using (18) and (19) in (20), follow the edge towards a destination.

C. Final Formation Controller

The final formation controller for the multi-agent system consists of two components: the gradient controller and the

TABLE III
CONTROL PARAMETERS FOR FIG 4

a_m	b_m	a_0	b_0	b_f	a_f	e_f
0.1	1.0	0.6	20.0	5.0	1.0	5.0

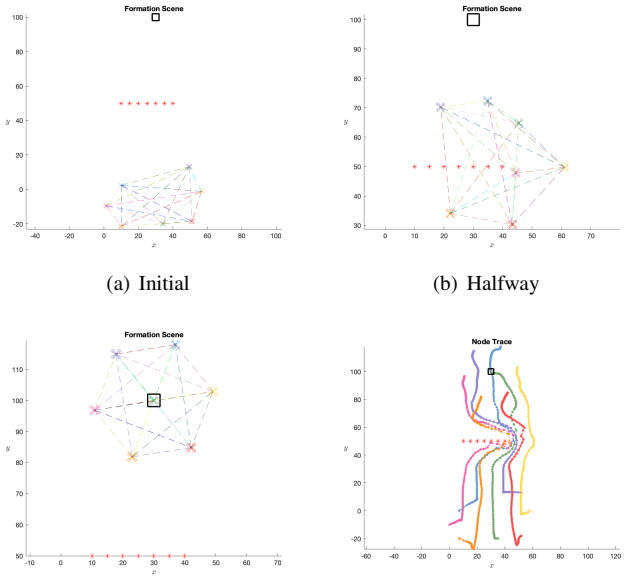

(a) Initial (b) Halfway

(c) Final (d) Trajectory

Fig. 4. Simulation of 7 UAVs following edge of jamming area while traveling toward the destination.

movement controller. We define the movement controller for agent i as $\mathcal{M}_i$, which is the overall behavior vector V_{movement} expressed as:

$$\mathcal{M}_i = V_{\text{movement}} = \begin{bmatrix} f_1(\cdot) & f_2(\cdot) & f_3(\cdot) \end{bmatrix} \begin{bmatrix} V_{\text{move\_to\_destination}} \\ V_{\text{jamming\_avoidance}} \\ V_{\text{follow\_edge}} \end{bmatrix} \tag{20}$$

The dynamics of the entire system can then be expressed as:

$$\begin{aligned} \dot{q}_i &= z_i \\ &= \underbrace{\sum_{j \in N_i} \left[\varphi(r_{ij}) \cdot e_{ij} \right]}_{\text{gradient controller}} \\ &\quad + \underbrace{\begin{bmatrix} f_1(\cdot) & f_2(\cdot) & f_3(\cdot) \end{bmatrix} \begin{bmatrix} V_{\text{move\_to\_destination}} \\ V_{\text{jamming\_avoidance}} \\ V_{\text{follow\_edge}} \end{bmatrix}}_{\text{movement controller}} \\ &= \mathcal{G}_i + \mathcal{M}_i. \end{aligned} \tag{21}$$

The gradient controller component is responsible for achieving the desired formation with maximum communication quality. The movement controller component is responsible for guiding the agents towards the goal while avoiding jamming area.

V. SIMULATION

In order to assess the performance of the final formation controller, a simulation was conducted. Inspiration for the final simulation came from [15]. The simulation involved 7 UAVs navigating toward a destination while avoiding a jamming area. The swarm has no prior knowledge about the location of the jamming area. The formation controller, which combines the gradient controller ($\mathcal{G}_i$) and the movement controller ($\mathcal{M}_i$), was employed to govern the agents' behavior.

TABLE IV
CONTROL PARAMETERS FOR FIG 6

a_m	b_m	a_0	b_0	a_f	b_f	e_f
0.1	1.0	0.6	20.0	1.0	0.0	5.0

The formation controller is used to create a control flow for an individual agent, illustrated in Fig 5. The behaviors of maximizing the communication quality and moving to the destination are constantly affecting the system during the simulation. Furthermore, there are three behaviors that can be triggered in the control flow. The first behavior occurs when an agent becomes isolated upon entering the jamming area. This isolated position is referred to as a jam location. Subsequently, the agent receives instructions to reverse its previous velocity, effectively undoing its last step. To mitigate the risk of potential live locks, an additional 10% of the distance is reversed. Once the agent's communication links are reconnected, it shares the coordinates of the jam location with the rest of the swarm. This triggers the jamming area avoidance for nearby agents as mentioned in (16). Lastly, the simulation ends when the centroid of the swarm is located in the destination square.

The simulation results, shown in Fig 6, demonstrate the progression of the swarm of UAVs over time. The sub-figures display the positions of the agents at different time intervals (in seconds), while the last sub-figure illustrates the trajectories followed by the agents.

VI. EVALUATION OF SIMULATION RESULTS

The average communication quality indicator, J_n, is calculated using (22). It represents the sum of the communication quality values $\varphi(r_{ij})$ between all neighboring agent pairs, divided by the total number of agent pairs. The average distance indicator, r_n, is determined using (23). It signifies the average distance between neighboring agents in terms of their positions r_{ij}.

$$J_n = \frac{\sum_{i=1}^{n} \sum_{j \in N_i} \phi(r_{ij})}{2n|N_i|}, \tag{22}$$

$$r_n = \frac{\sum_{i=1}^{n} \sum_{j \in N_i} r_{ij}}{2n|N_i|}, \tag{23}$$

Fig 7 presents the evaluation results for the simulation depicted in Fig 6. The left sub-figure displays the trend of the average distance indicator r_n over time, while the right

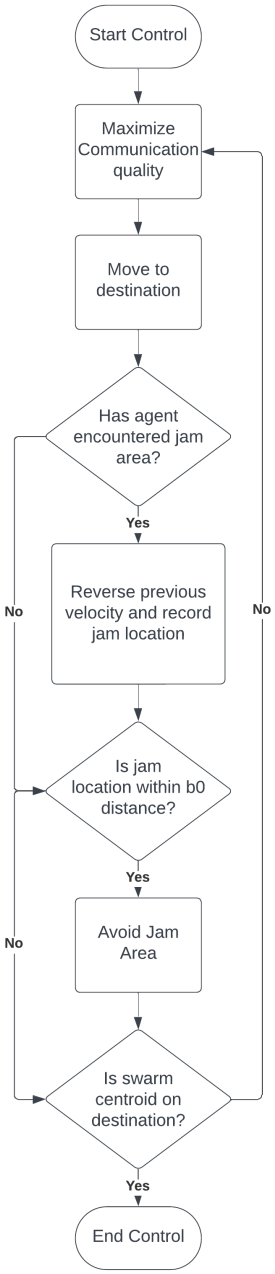

Fig. 5. Control flow illustrating the control loop implementation for the final simulation.

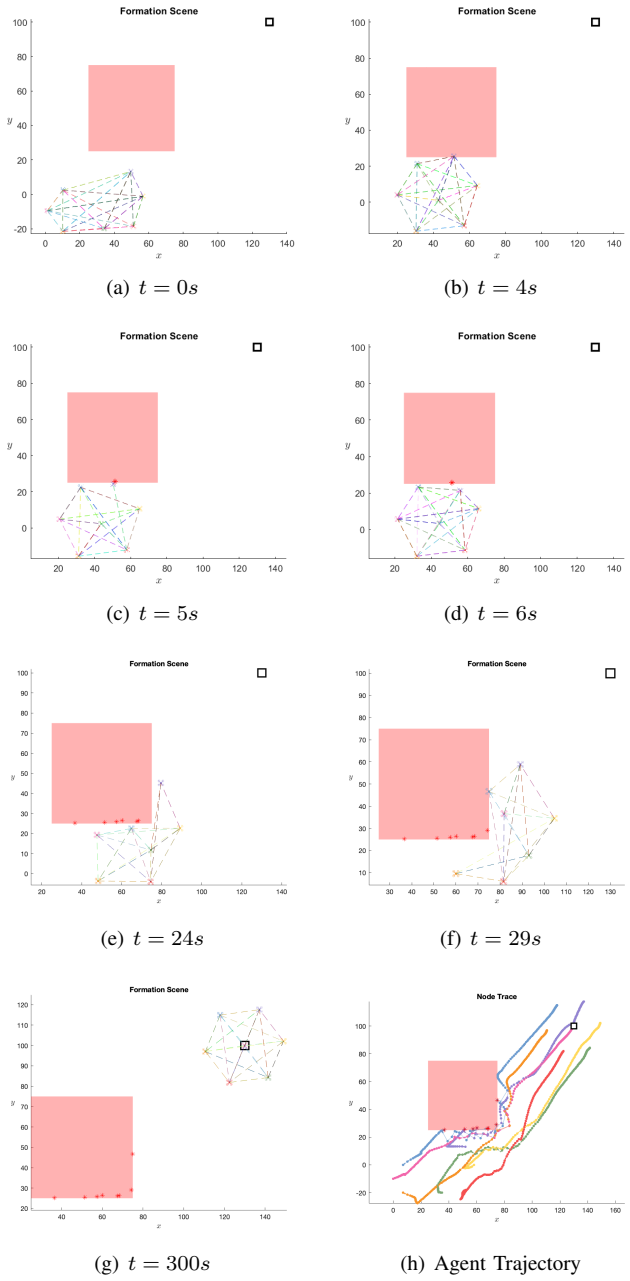

(a) $t = 0s$ (b) $t = 4s$ (c) $t = 5s$ (d) $t = 6s$ (e) $t = 24s$ (f) $t = 29s$ (g) $t = 300s$ (h) Agent Trajectory

Fig. 6. Simulation of 7 UAVs achieving jamming area avoidance while traveling toward the destination.

sub-figure illustrates the trend of the average communication quality indicator J_n over time.

From the evaluation results, it can be observed that the average communication quality indicator decreases and then reaches a steady state. This decrease is attributed to the jamming area, which affects the communication between neighboring agents. However, as the swarm adapts its behavior and employs the movement controller ($\mathcal{M}_i$), the average communication quality gradually improves and starts to recover.

Similarly, the average distance indicator (r_n) initially exhibits fluctuations as the swarm navigates and avoids the jamming area. Eventually, the average distance converges to an optimal value over time, indicating that the agents maintain a relatively stable distance from their neighbors.

VII. Conclusion

In conclusion, the proposed formation control strategy successfully enables a swarm of UAVs to achieve efficient navigation towards a destination while avoiding a jamming area. By integrating the gradient controller for the formation and the movement controller for jamming area avoidance, the swarm

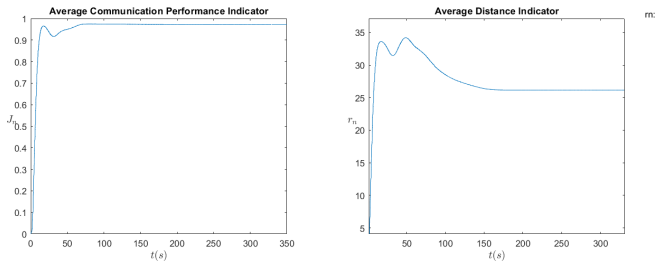

(a) (b)

Fig. 7. Evaluation for simulation in Fig 6. (a) Average communication quality indicator for the overall system. (b) Average distance indicator for overall system

exhibits adaptive behavior, which maintains communication quality and desired formation. The simulation results demonstrate the effectiveness of the approach in achieving these objectives. The current approach exhibits certain limitations, primarily concerning the fixed direction in which agents maneuver around jamming locations. Additionally, more complex path planning could be implemented by adding many destination points serving as checkpoints to guide the swarm through more complex environments. Efforts aimed at improving the impact of avoiding jamming areas on communication quality hold promising potential for further advancements. Further research and experimentation can build upon these findings to enhance swarm coordination and navigation in complex environments.

ACKNOWLEDGMENT

This research was supported by the National Science Foundation under Grant No. 2150213.

REFERENCES

[1] Z. Fu, T. Yang, and J. Wang, "Effects of jamming on a multi-agent flocking model with distributed estimation of global features," in *2016 Future Technologies Conference (FTC)*. IEEE, 2016, pp. 622–625.

[2] H. Li, J. Peng, W. Liu, K. Gao, and Z. Huang, "A novel communication-aware formation control strategy for dynamical multi-agent systems," *Journal of the Franklin Institute*, vol. 352, no. 9, pp. 3701–3715, 2015.

[3] D. Xu, X. Zhang, Z. Zhu, C. Chen, P. Yang *et al.*, "Behavior-based formation control of swarm robots," *mathematical Problems in Engineering*, vol. 2014, 2014.

[4] T. Liu, J. Huang, J. Guo, and Y. Shan, "Survey on anti-jamming technology of uav communication," in *International Conference on 5G for Future Wireless Networks*. Springer, 2022, pp. 111–121.

[5] L. Chen, "On selfish and malicious behaviors in wireless networks-a non-cooperative game theoretic approach," Ph.D. dissertation, Télécom ParisTech, 2008.

[6] W. Xu, T. Wood, W. Trappe, and Y. Zhang, "Channel surfing and spatial retreats: defenses against wireless denial of service," in *Proceedings of the 3rd ACM workshop on Wireless security*, 2004, pp. 80–89.

[7] Y. Zhao, Y. Hao, Q. Wang, and Q. Wang, "A rigid formation control approach for multi-agent systems with curvature constraints," *IEEE Transactions on Circuits and Systems II: Express Briefs*, vol. 68, no. 11, pp. 3431–3435, 2021.

[8] S. Xing, T. Yang, and H. Song, "Consensus-based communication-aware formation control for a mobile multi-agent system," in *SoutheastCon 2023*. IEEE, 2023, pp. 60–67.

[9] A. Durniak, "Welcome to ieee xplore," *IEEE Power Engineering Review*, vol. 20, no. 11, p. 12, 2000.

[10] R. Olfati-Saber, "Flocking for multi-agent dynamic systems: Algorithms and theory," *IEEE Transactions on automatic control*, vol. 51, no. 3, pp. 401–420, 2006.

[11] C. Li, Z. Qu, and M. A. Weitnauer, "Distributed extremum seeking and formation control for nonholonomic mobile network," *Systems & Control Letters*, vol. 75, pp. 27–34, 2015.

[12] A. Goldsmith, *Wireless communications*. Cambridge university press, 2005.

[13] H. Li, J. Peng, X. Zhang, and Z. Huang, "Flocking of mobile agents using a new interaction model: A cyber-physical perspective," *IEEE Access*, vol. 5, pp. 2665–2675, 2017.

[14] T. Balch and R. C. Arkin, "Behavior-based formation control for multirobot teams," *IEEE transactions on robotics and automation*, vol. 14, no. 6, pp. 926–939, 1998.

[15] B. Duan, D. Yin, Y. Cong, H. Zhou, X. Xiang, and L. Shen, "Anti-jamming path planning for unmanned aerial vehicles with imperfect jammer information," in *2018 IEEE International Conference on Robotics and Biomimetics (ROBIO)*. IEEE, 2018, pp. 729–735.